Insulin-degrading Enzyme Regulates the Proliferation and Apoptosis of Porcine Skeletal Muscle Stem Cells via Myostatin/MYOD Pathway

Bingyuan Wang
Chinese Academy of Agricultural Sciences Institute of Animal Science https://orcid.org/0000-0003-0970-8024

Jiankang Guo
Chinese Academy of Agricultural Sciences Institute of Animal Science

Mingrui Zhang
Chinese Academy of Agricultural Sciences Institute of Animal Science

Zhiguo Liu
Chinese Academy of Agricultural Sciences Institute of Animal Science

Rong Zhou
Chinese Academy of Agricultural Sciences Institute of Animal Science

Fei Guo
China Agricultural University College of Animal Science and Technology

Kui Li (likui@caas.cn)
Chinese Academy of Agricultural Sciences Institute of Animal Science

Yulian Mu
Chinese Academy of Agricultural Sciences Institute of Animal Science

Research

Keywords: insulin-degrading enzyme (IDE), pig, skeletal muscle stem cells, proliferation and apoptosis, myostatin (MSTN)

Posted Date: March 26th, 2021

DOI: https://doi.org/10.21203/rs.3.rs-361389/v1

Abstract

Background: Identifying the genes relevant for muscle development is pivotal to improve meat production and quality in pigs. Insulin-degrading enzyme (*IDE*), a thiol zinc-metalloendopeptidase, has been known to regulate the myogenic process of mouse and rat myoblast cell lines, while its myogenic role in pigs remained elusive. Therefore, the current study aimed to identify the effects of *IDE* on the proliferation and apoptosis of porcine skeletal muscle stem cells and underlying molecular mechanism.

Results: We found in the present study that *IDE* was widely expressed in porcine tissues, including kidney, lung, spleen, liver, heart, and skeletal muscle. Then, to explore the effects of *IDE* on the proliferation and apoptosis of porcine skeletal muscle stem cells, we subjected the cells to siRNA-mediated knockdown of *IDE* expression, which resulted in promoted cell proliferation and reduced apoptosis. As one of key transcription factors in myogenesis, *MYOD*, its expression was also decreased with *IDE* knockdown. To further elucidate the underlying molecular mechanism, RNA sequencing was performed. Among transcripts perturbed by the *IDE* knockdown after, a down-regulated gene myostatin (*MSTN*) which is known as a negative regulator for muscle growth attracted our interest. Indeed, *MSTN* knockdown led to similar results as those of the IDE knockdown, with upregulation of cell cycle-related genes, downregulation of *MYOD* as well as apoptosis-related genes, and enhanced cell proliferation.

Conclusion: Our findings suggest that *IDE* regulates the proliferation and apoptosis of porcine skeletal muscle stem cells through *MSTN/MYOD* pathway. Thus, we recruit *IDE* to the gene family of regulators for porcine skeletal muscle development, and propose *IDE* as an example of gene to prioritize in order to improve pork production.

Introduction

Skeletal myogenesis is a complex process, which sequentially involves the proliferation of myoblasts, withdrawal from cell cycle, differentiation into mononucleated myocytes, fusion of myocytes into multinucleated myotubes, and maturation of myotubes into mature muscle fibers [1]. Defective muscle development is responsible for several complex humans diseases[2], exemplifying the importance of preserving muscle formation and/or regeneration via e.g. adequate physical activity and metabolic health. In animal species, including pigs and other meat livestock, skeletal muscle provides a source of protein for human nutrition, and the extent of muscle development directly affects their commercial value [3]. Against this background, it is of great importance to illuminate the molecular regulators of skeletal myogenesis, with a long-term aim to improve the treatment of muscle deficiency-related diseases and pig breeding.

Extensive studies have documented that myogenic regulatory factors (MRFs), MyoD (myogenic determination factor 1), Myog (myogenin), Myf5 (muscle regulatory factor 5), and MRF4 (muscle regulatory factor 4), coordinately function in different stages of muscle cell fate and play central roles in myogenesis [4]. Chronologically, the factors MyoD and Myf5 operate earlier to establish the muscle

lineage, by participating in the commitment and proliferation of myogenic-directed cells. MyoD and Myf5 are followed by MyoG expression, which controls the differentiation process, and lastly by MRF4, which is involved in myotube maturation [5, 6] [7]. Of these four MRFs, MyoD was the first one identified as a myogenic factor since forced expression of MyoD converted fibroblasts to stable myoblasts and activated muscle-specific genes [8, 9]. Next to MyoD, gene family member MyoG was also identified as a factor regulating myogenesis, since transfection of MyoG into mesenchymal cell line produced cells expressing muscle-specific markers [10]. Both Myf5 and MRF4 act upstream of Myod to direct embryonic multipotent cells into the myogenic lineage [11], which implied the importance of MyoD as a downstream effector in myogenesis.

Unlike the downstream effectors, what lies upstream in the myogenic regulatory cascade is less well defined. Among potential candidates, the insulin degrading enzyme (IDE) was shown to play a relevant role in mouse and rat cell lines. Inhibition of IDE sustained the proliferation of C2C12 myoblasts and blocked the differentiation of C2C12 and L6 myoblasts [12, 13]. IDE is a neutral zinc and thio-dependent metallopeptidase which belongs to the M16 (pitrilysin) family of zinc-metallo-endopeptidases, namely inverzincins. IDE is present in humans and in all eukaryotes and bacteria, displaying in all species a surprisingly highly conserved primary sequence [14]. The biological role of IDE has long been associated with Alzheimer's disease (AD) and type 2 diabetes mellitus (DM2) due to its well-known substrates amyloid beta-protein (Abeta) and insulin [15, 16]. IDE controlled the translocation of insulin to the cell nucleus, playing a crucial role in insulin's regulation of gene expression and cell proliferation [17]. The IDE knockout mice showed increased cerebral accumulation of endogenous Abeta, a hallmark of AD, and had hyperinsulinemia and glucose intolerance, hallmarks of DM2 [18]. In addition, IDE knockout mice also presented reduced testes weight, reduced seminiferous tubules diameter, and reduced sperm quality (including decreased sperm viability and morphology) compared to wild type mice [19].

In the present study, we tested the role of IDE in the proliferation of porcine skeletal muscle stem cells (PSMSCs) and the underlying molecular mechanism, aiming to better understand the molecular regulation of porcine muscle development and prioritize candidate factors for the improvement of meat production. Using a knockdown model we established that albeit IDE was widely expressed in porcine tissues, its downregulation in PSMSCs promoted cell proliferation and counteracted apoptosis via myostatin (MSTN)/MYOD pathway.

Materials And Methods

Pig tissue samples

All animals were treated humanely according to criteria outlined in the “Guide for the Care and Use of Laboratory Animals” published by the Institute of Animal Sciences, Chinese Academy of Agricultural Sciences (Beijing, China). Procedures were approved by the Animal Care and Use Committee (IAS20160616). Pigs (*Sus scrofa*) were slaughtered following the Animal Care Guidelines of the Ethics committee of Chinese Academy of Agricultural Sciences. Tissue samples including kidney, lung, spleen,

liver, heart, and muscle of three 180-day old male large white pigs were collected and kept in liquid nitrogen until further processing.

Cell culture and transfection

Porcine skeletal muscle stem cells (PSMSCs) were purchased from iCell (iCell-0017a, Shanghai, China). Cells were cultured in high-glucose Dulbecco's modified Eagle's medium (DMEM) supplemented with 10% fetal bovine serum (FBS, Gibco) at 37 °C in a humidified incubator containing 5% CO_2. The siRNAs of insulin-degrading enzyme (IDE) (target sequence: GGAATGAAGTTCACAATAA) and MSTN (target sequence: CTCCTAACATTAGCAAAGA) were designed and synthesized by RiboBio (Guangzhou, China). Transfections were performed as previously using Lipofectamine RNAiMAX reagent (Invitrogen) according to the manufacturer's instructions. Briefly, 1 x 10^5 cells were seeded in each well of a six-well plate and cultured overnight. Next day cells were transfected with 50 mM siRNA. After 48 h of transfection, the cells were collected for further analysis.

Real-time quantitative polymerase chain reaction (RT-qPCR)

Total RNA was extracted from pig tissues and PSMSCs using TRIzol reagent (Invitrogen). 1 μg RNA was reverse transcribed to cDNA using PrimeScript™ RT reagent kit with gDNA eraser (TaKaRa, Cat. # RR047A) according to the manufacturer's instructions. RT-qPCR was performed in a final volume of 20 μL which contained 10 μL SYBR® Premix Ex Taq™ (2x; TaKaRa, Cat. # RR420A), 1 μL cDNA, 0.4 μL forward primer (10 μM), 0.4 μL reverse primer (10 μM), 0.4 μL ROX reference dye II, and 7.8 μL sterile distilled H2O on an ABI 7500 Fast Real-Time PCR system (Applied Biosystem). Glyceraldehyde-3-phosphate dehydrogenase (GAPDH) was used as a reference gene. Relative mRNA expression was determined by normalizing target gene expression against GAPDH expression and using 2^{-ddct} method [20]. The primer sequences used for RT-qPCR were shown in additional file 1. Results are presented as fold changes relative to the control.

Western blotting analysis

Total proteins were extracted from pig tissues and PSMSCs using protein extraction reagent containing protease and phosphatase inhibitor (Thermo Scientific). Equal amount of denatured proteins was separated by 10% SDS-PAGE and then transferred to nitrocellulose membranes (Millipore). Thereafter, the membranes were blocked with 5% nonfat milk for 1 h at room temperature followed by primary antibodies incubation overnight at 4°C. The primary antibodies were anti-IDE (1:1000, ab33216), anti-MSTN (1:1000, ab201954) (Abcam), anti-MYOD (1:500, sc-377460) (Santa Cruz Biotechnology), anti-PCNA (1:1000, Cell Signaling Technology, 2586), anti-CCNE1 (1:1000, Cell Signaling Technology, 4129), anti-P53 (1:800, Cell Signaling Technology, 2524), anti-BAX (1:500, Cell Signaling Technology, 2772), anti-BCL2 (1:500, Cell Signaling Technology,3498), and anti-GAPDH (1:1000, Cell Signaling Technology, 2118). HRP-conjugated secondary antibodies were used to incubate the membranes for 1 h at room temperature. The blots were developed using Pierce ECL Western Blotting Substrate according to the

manufacturer's instructions (Pierce). The protein bands were visualized on a Tanon-5200 Chemiluminescent Imaging System (Shanghai, China) and quantified via calculating integrated density with ImageJ software. The protein expression was normalized to endogenous GAPDH.

Cell proliferation assay

The viability of PSMSCs was tested using Cell Counting Kit 8 (CCK-8) (Dojindo Molecular Technologies) according to the manufacturer's instructions. Briefly, the cells were seeded at a density of 2000 cells per well in 96-well plate and cultured overnight. Then, the cells were treated with siRNAs for 48 h. Thereafter, 10 μl CCK-8 solution was added to each well and incubated at 37°C for 1 h. The absorbance was measured by a microplate reader (Molecular Devices, SpectraMax M5, USA) at the wavelength of 450 nm. The cell viability (%) was calculated with the equation (Absorbance of experimental group – Absorbance of blank)/ (Absorbance of control group – Absorbance of blank) *100. Besides cell viability, the proliferation of PSMSCs was also tested through cell counting. Briefly, the cells were trypsinized after siRNA transfection 48 h, and then counted using a cell counter (JIMBIO CL, China).

RNA sequencing (RNA-seq)

Total RNA was extracted from PSMSCs (two groups, each with three biological replicates) using TRIzol reagent (Invitrogen). 2 μg RNA per sample was used for the following steps which were performed by Novogene Co., Ltd. (Beijing, China). Sequencing libraries were generated using NEVNext® Ultra™ RNA Library Prep Kit for Immumina® (NEB, USA) following manufacturer's instructions. The library quality was assessed on the Agilent Bioanalyzer 2100 system and the library preparations were sequenced on an Immumina Novaseq platform and 150 bp paired-end reads were generated.

RNA-seq data analysis

Raw data (raw reads) of fastq format were firstly processed. Clean reads were obtained by removing reads containing adapter, reads containing ploy-N and low quality reads from raw data. Q20, Q30 and GC content of the clean data were calculated. The following analyses were all based on the clean reads with high quality scores. Hisat2 was selected as the mapping tool.

FeatureCounts v1.5.0-p3 was used to count the reads numbers mapped to each gene. And then Fragments Per Kilobase of transcript sequence per Millions base pairs sequenced of each gene was calculated based on the length of the gene and reads count mapped to this gene. Differential expression analysis between control groups and treated-groups (two biological replicates per condition) was performed using the DESeq2 R package (1.16.1). The resulting P-values were adjusted using the Benjamini and Hochberg's approach for controlling the false discovery rate. The differentially expressed genes (DEGs) were defined as those genes with an adjusted P-value <0.05 and a |log2(FoldChange)| > =1.

Gene Ontology (GO) enrichment analysis and Kyoto Encyclopedia of Genes and Genomes (KEGG) enrichment analysis of DEGs were implemented by the clusterProfiler R package, in which gene length

bias was corrected. The ENTREZ gene IDs were inputted, and genome-wide annotation for pig was obtained by the “org.Ss.eg.db”package. The GO enrichment analysis was performed by the enrichGO function, in which DEGs were divided into three groups: molecular function (MF), cellular component (CC), and biological process (BP). The enrichKEGG function was used for KEGG pathways enrichment analysis. An adjusted P-value <0.05 was considered for significantly enriched GO terms and KEGG pathways.

Statistical analysis

Data were analyzed using GraphPad Prism 5 and presented as mean ± standard deviation (SD). The statistical significance was calculated from at least three independent experiments using Student’s two-tailed paired and unpaired t-test. $P < 0.05$ was considered significant.

Results

The expression of *IDE* in pig tissues

To determine the expression of *IDE* in pig tissues, mRNA was isolated from kidney, lung, spleen, liver, heart, and skeletal muscle of adult large white pigs and subjected to RT-qPCR. Overall, *IDE* was extensively expressed in these tissues (Figure 1 A-C). In detail, relative mRNA levels of IDE were higher in kidney, lung, spleen, and liver, compared to those in heart and skeletal muscle (Figure 1A). Consistent with the results of RT-qPCR, western blotting analysis showed relatively higher level of IDE protein in kidney, lung, and spleen, and relatively lower level in liver, heart, and skeletal muscle (Figure 1B and 1C). These concordant findings suggested that *IDE* gene was extensively expressed in multiple tissues of pigs; its expression was regulated to attain different levels in different tissues, and thus might play important roles in pig development.

IDE knockdown reduces the expression of *MYOD*

As key transcription factors in myogenesis, *MYOD* regulates transcription of the majority of muscle-specific genes. Thus, to elucidate the possible effect of *IDE* in myogenesis, we tested its impact on *MYOD* expression following *IDE* knockdown using IDE siRNA (IDEsi). The efficacy of *IDE* knockdown was confirmed by RT-qPCR (Figure 1D) and western blotting (Figure 1E and 1F). Compared to negative control siRNA (NC) group, *MYOD* expression was reduced at both the mRNA (Figure 1D) and protein level (Figure 1E and 1F) in the *IDE* knockdown group. These results supported that *IDE* might play certain roles in porcine skeletal muscle development.

Downregulation of *IDE* promotes the proliferation of porcine skeletal muscle stem cells (PSMSCs)

Skeletal muscle stem cells play important roles in muscle development and injury-induced muscle regeneration through their proliferation and differentiation. Therefore, building on our previous observation that IDE was necessary to sustain *MYOD* expression, we asked whether *IDE* silencing would affect the proliferation of PSMSCs. To this end, we performed cell proliferation analyses using CCK-8

assay and cell number counting. CCK-8 assay revealed that downregulation of *IDE* significantly enhanced cell viability after transfection for 24 h, 48 h, and 72 h ($P<0.001$, $P < 0.01$, and $P < 0.01$, respectively) (Figure 2A). Consistent with the improved cell viability, also the number of PSMSCs was significantly increased after downregulation of *IDE* as measured after transfection for 24 h, 48 h, and 72 h ($P<0.05$, $P < 0.01$, and $P < 0.05$, respectively) (Figure 2B). The relative expression of cell cycle-related genes *PCNA* and *CCNE1* was increased in IDEsi group than that in NC group, both at the mRNA and protein level (Figure 2C-E). Collectively, these findings indicated that *IDE* negatively regulated the proliferation of PSMSCs.

IDE inhibition mitigates the apoptosis of PSMSCs

Having identified the negative regulatory role of *IDE* in the proliferation of PSMSCs, we tested whether *IDE* inhibition would mitigate the apoptosis of PSMSCs. The expression of apoptosis-related genes was examined by RT-qPCR and western blotting. While *IDE* inhibition had no impact on the mRNA expression of *BCL2,* compared to NC group, it significantly decreased the mRNA expression of *BAX* and *P53* ($P < 0.01$) (Figure 2F). Protein levels of BCL2, BAX and P53 were consistent with those of the cognate mRNA (Figure 2G and 2H), thereby establishing that *IDE* inhibition mitigated the apoptosis of PSMSCs.

Differentially expressed genes (DEGs) are screened by RNA sequencing (RNA-seq)

To uncover the molecular mechanism underlying the effect of *IDE* knockdown in PSMSCs, we conducted RNA-seq analysis to compare the transcriptomes between IDEsi-transfected (IDEsi group) and mock-transfected PSMSCs (NCsi group). A total of 627 mRNAs were differentially expressed (adjusted $P<0.05$, $|\log2 \text{ fold change}| >=1$), including 168 upregulated and 459 downregulated DEGs in IDEsi group compared to NCsi group (Figure 3A and 3B). The top 20 up-regulated genes which included *IDE* and the top 20 down-regulated genes are shown, respectively, in Table 1 and Table 2, where they are ranked by log2 fold change. To validate RNA-seq results, we subjected a subset of 28 randomly selected DEGs to RT-qPCR. Up-regulated DEGs (including *RHCG*, *ISG12(A)*, *LOC100513671*, *RSAD2*, *ANXA8*, *NUPR1*, *RENBP*, *USP18;* Figure 3C) and down-regulated DEGs (including *CENPF*, *LRRC17*, *KIF11*, *TOP2A*, *NEB*, *TUBB6*, *DES*, *SEMA3D*, *TNC*, *MYBL2*; Figure 3D) were confirmed. With the comfort of this validation, we undertook a gene ontology (GO) analysis of the DEGs and each top 10 terms of biological process, cellular component, and molecular function were shown in Figure 3E. Further analysis revealed significant enrichment in 11 biological process terms from down-regulated DEGs (adjusted $P<0.05$) (Table 3), which included muscle organ development. Further, Kyoto Encyclopedia of Genes and Genomes (KEGG) enrichment analysis of these DEGs revealed 8 significantly enriched pathways, including cell cycle and DNA replication (adjusted $P<0.05$) (Figure 3F). Thus, the results of DEGs pointed at candidate genes for the molecular mechanism of *IDE* function in PSMSCs.

Table 1 Top 20 up-regulated differentially expressed genes

Gene Name	Gene ID	log2 Fold Change	P (adj)
LOC102165015	102165015	3.870998142	0.002158876
SLC5A7	100512044	3.371005733	5.96E-28
C2CD4C	110259383	3.207169998	0.000587205
MUC12	100286744	2.683796274	1.36E-06
SHC2	110259382	2.435089173	0.023407752
LOC100737730	100737730	2.381840904	0.031178933
HRK	100155596	2.34884663	7.78E-16
SERPINB5	100155836	2.310033525	3.39E-07
TLR4	399541	2.302003156	0.000464508
SCIN	100512981	2.251388026	8.55E-05
PDK4	100286778	2.135906406	0.036212786
LOC106504682	106504682	2.130392455	0.015514156
RHCG	733644	2.121055358	2.67E-152
NKPD1	110261005	2.114110507	0.037505405
SLPI	396886	2.08260702	6.95E-06
LOC110257938	110257938	2.07336763	4.82E-09
CDH8	100625758	2.06017948	0.002443282
WHRN	100520475	2.027474023	0.011737607
LOC110261055	110261055	1.966638858	0.023394409
CASP14	100518472	1.954093983	8.62E-09

P (adj) <0.05 is considered statistical significance.

Table 2 Top 20 down-regulated differentially expressed genes

Gene Name	Gene ID	log2 Fold Change	P (adj)
KCNA1	100048962	-3.718882073	0.003586753
CPLX1	100624856	-3.410876944	0.003637539
LOC100157763	100157763	-3.396882421	0.003520403
HPGD	100156186	-2.97555016	0.002289409
LYPD5	100626406	-2.827359184	6.63E-17
GALP	396772	-2.789892579	0.007082538
GAL	397465	-2.731537614	0.010545262
XIRP2	397689	-2.602960594	2.44E-103
CLDN9	100302022	-2.541575532	8.67E-05
PTGDR2	100510947	-2.522357235	0.001139225
LOC110260209	110260209	-2.488926485	0.029408964
KCNA3	100156614	-2.454171147	0.000614147
PCSK9	100620501	-2.355200193	0.018361228
IDE	100155309	-2.336970662	2.59E-190
COL13A1	100157199	-2.301938419	0.001092127
MSTN	399534	-2.255207455	3.81E-11
LOC102165115	102165115	-2.230630904	0.030565317
LOC106510075	106510075	-2.198719453	1.35E-07
XKR5	100524909	-2.159402704	7.11E-07
SCN3A	100625056	-2.143679978	0.0291151

P (adj) <0.05 is considered statistical significance.

Table 3. Significant enrichment in GO terms

Category	GO ID	Description	P (adj)
BP	GO:0000280	nuclear division	0.022
BP	GO:0007067	mitotic nuclear division	0.022
BP	GO:0043902	positive regulation of multi-organism process	0.022
BP	GO:0000278	mitotic cell cycle	0.022
BP	GO:0048285	organelle fission	0.022
BP	GO:1903047	mitotic cell cycle process	0.023
BP	GO:0090068	positive regulation of cell cycle process	0.027
BP	GO:0010564	regulation of cell cycle process	0.029
BP	GO:0007517	muscle organ development	0.037
BP	GO:0030154	cell differentiation	0.047
BP	GO:0051301	cell division	0.047

BP: biological process. P (adj) <0.05 is considered statistical significance.

IDE regulates PSMSCs through myostatin (*MSTN*)/*MYOD* pathway

Among the DEGs we singled out *MSTN* because it is well known to negatively regulate muscle development and it was downregulated in the IDEsi group compared to NC group (Table 2). To determine whether *IDE* regulated the proliferation of PSMSCs through *MSTN*, we first verified the downregulation of *MSTN* after IDEsi treatment via RT-qPCR and western blotting (Figure 4A-C). Next, we interfered with the expression of *MSTN* using MSTN siRNA, observing that cell viability was increased compared with NC group ($P < 0.01$) (Figure 4D). Likewise, the protein level of MYOD was reduced with declined MSTN protein level (Figure 4E and 4F). In addition, *MSTN* knockdown increased the expression of cell cycle-related gene CCNE1 while it decreased the expression of apoptosis-related gene BAX (Figure 4G and 4H). Thus, these findings uncovered the similar effect of *IDE* and *MSTN* in the proliferation and apoptosis in PSMSCs, which suggested that *IDE* regulated PSMSCs through *MSTN/MYOD* pathway.

Discussion

In contrast to clear roles played in AD and DM2 pathologies [21] and in male reproduction [19], the role of *IDE* remains hypothetical in muscle development, as suggested by studies in mouse and rat myoblast cell lines [12, 13]. Given the commercial value and the importance of pig in biomedicine, we designed the present study to test the role of *IDE* in porcine skeletal muscle stem cells (PSMSCs). Our results contribute to a better understanding of the molecular mechanisms of porcine muscle development, and also provide candidate genes for improving pork production.

We first detected the expression of *IDE* in multiple tissues of large white pigs. Although *IDE* was purified from pig skeletal muscle in an earlier study [22], this is the first time that *IDE* expression has been assessed in multiple porcine tissues at once. We found that *IDE* was widely expressed in the tested tissues (kidney, lung, spleen, liver, heart, and skeletal muscle), and relatively higher expression was shown in kidney, lung, and spleen compared to heart and skeletal muscle. Previous studies reported that *IDE* mRNA was highly abundant in kidney and liver of rat [23], and IDE protein was extensively expressed in human tissues, including kidney, liver, lug, brain, and muscle [24]. The similar expression pattern of *IDE* in different species, but at different levels in different tissues, imply conservation of primary sequence and functional roles.

The development of skeletal muscle is closely related to the health of human and the commercial value of meat livestock, suggesting the importance of myogenesis-related studies. *IDE* was reported as playing importantly regulatory role in mouse myoblasts, since inhibition of *IDE* as well as knockdown of *IDE* mRNA sustained mouse myoblast proliferation [13]. It is known that myogenesis is a complex process in which the myoblasts proliferate and exit from cell cycle to start differentiation. As the proliferating progeny of satellite cells, the myoblasts express MyoD and Myf5 and undergo multiple rounds of cell division [25]. It is known that the proliferation of skeletal muscle stem cells was promoted through keeping MyoD expression at low levels [26]. MyoD deficiency in satellite cells caused them remaining in proliferative state [27]. MyoD-null myoblasts were more resistant to apoptosis during proliferation [28]. In our study, inhibiting *IDE* expression by siRNA transfection impeded the expression of *MYOD*, promoted the proliferation and attenuated the apoptosis of PSMSCs. Cell proliferation markers *PCNA* and *CCNE1* were also increased after *IDE* inhibition. Therefore, the reduced *MYOD* expression that followed to *IDE* inhibition might contribute to the enhanced proliferation and ameliorated apoptosis of PSMSCs.

To illuminate the molecular bases of *IDE* function in PSMSCs, we applied RNA sequencing (RNA-seq), comparing IDE knocked down PSMSCs and control PSMSCs. The RNA-seq data analysis identified 2658 up-regulated and 2536 down-regulated genes in the IDE knockdown group compared to control. As expected, *IDE* was one of the top 20 down-regulated genes. Interestingly, we found that myostatin (*MSTN*) was also one of top 20 down-regulated genes. *MSTN*, a member of transforming growth factor beta (TGF-beta) superfamily, has been reported as a negative regulator of muscle growth and development [29-33]. Numerous studies revealed that loss-of-function mutation of *MSTN* led to double-muscling phenotypes in livestock, including cattle, pig, sheep, and goat [34-40], which made *MSTN* a popular candidate gene for animal breeding of improving meat production. *MSTN* operates in muscle development by inhibiting the proliferation and differentiation of myoblast [41, 42]. Thus we posited that *IDE* would regulate the proliferation and apoptosis through *MSTN*. Our knockdown experiment showed that *MSTN* promoted the proliferation of PSMSCs. Furthermore, *MSTN* inhibition also decreased the protein expression of MYOD and BAX, but increased the expression of CCNE1, which exhibited similar results with *IDE* knockdown. These results suggested that 1) *IDE* regulated the proliferation and apoptosis through *MSTN/MYOD* pathway, and 2) *IDE* is a crucial regulator of porcine muscle development and a new candidate for the improvement of pork meat production.

Conclusions

In summary, we discovered that *IDE* was extensively expressed in adult pig tissues, including kidney, lung, spleen, liver, heart, and skeletal muscle. Further functional assessments revealed that *IDE* knockdown promoted the proliferation and mitigated the apoptosis of porcine skeletal muscle stem cells, which was regulated through *IDE/MSTN/MYOD* pathway. Thus, we recruit *IDE* to the gene family of regulators for porcine skeletal muscle development, implying *IDE* as a candidate gene for the improvement of pork production.

Abbreviations

IDE: Insulin-degrading enzyme; MYOD: myogenic determination factor 1; MSTN: myostatin; MRFs: myogenic regulatory factors; Myog: myogenin; Myf5: muscle regulatory factor 5; MRF4: muscle regulatory factor 4; AD: Alzheimer's disease; DM2: type 2 diabetes mellitus; Abeta: amyloid beta-protein; PSMSCs: porcine skeletal muscle stem cells.

Declarations

Acknowledgements

The authors are grateful to all the staff who helped in this study from the group and institute.

Authors' contributions

BYW and YLM conceived, designed the experiments, wrote the manuscript, obtained the finance supports; JKG and MRZ mainly performed the experiments; ZGL, RZ, and FG prepared samples, analyzed data; KL revised the manuscript and obtained the finance supports. All authors read and approved the final manuscript.

Funding

This work was supported by the Special Fund of Chinese Central Government for Basic Scientific Research Operations in Commonweal Research Institutes (2020-YWF-YB-06), the National Transgenic Breeding Project (2016ZX08006001), and the Agricultural Science and Technology Innovation Program (ASTIP-IAS05).

Availability of data and materials

All data generated or analyzed during this study are available from the corresponding authors on reasonable request.

Ethics approval and consent to participate

All procedures conducted in the present study were approved by the Animal Care and Use Committee of Institute of Animal Sciences, Chinese Academy of Agricultural Sciences (ID: IAS20160616)

Consent for publication

Not applicable.

Competing interests

The authors declare that they have no conflict of interest.

References

1. Chal J, Pourquié O. Making muscle: skeletal myogenesis in vivo and in vitro. Development. 2017;144(12):2104-2122.
2. Huh MS, Smid JK, Rudnicki MA. Muscle function and dysfunction in health and disease. Birth defects research Part C, Embryo today : reviews. 2005;75(3):180-192.
3. Jan AT, Lee EJ, Ahmad S, Choi I. Meeting the meat: delineating the molecular machinery of muscle development. Journal of animal science and technology. 2016;58:18.
4. Asfour HA, Allouh MZ, Said RS. Myogenic regulatory factors: The orchestrators of myogenesis after 30 years of discovery. Experimental biology and medicine (Maywood, NJ). 2018;243(2):118-128.
5. Rawls A, Valdez MR, Zhang W, Richardson J, Klein WH, Olson EN. Overlapping functions of the myogenic bHLH genes MRF4 and MyoD revealed in double mutant mice. Development. 1998;125(13):2349-2358.
6. Kitzmann M, Fernandez A. Crosstalk between cell cycle regulators and the myogenic factor MyoD in skeletal myoblasts. Cell Mol Life Sci. 2001;58(4):571-579.
7. Yamamoto M, Legendre NP, Biswas AA, Lawton A, Yamamoto S, Tajbakhsh S, et al. Loss of MyoD and Myf5 in Skeletal Muscle Stem Cells Results in Altered Myogenic Programming and Failed Regeneration. Stem cell reports. 2018;10(3):956-969.
8. Davis RL, Weintraub H, Lassar AB. Expression of a single transfected cDNA converts fibroblasts to myoblasts. Cell. 1987;51(6):987-1000.
9. Weintraub H, Tapscott SJ, Davis RL, Thayer MJ, Adam MA, Lassar AB, et al. Activation of muscle-specific genes in pigment, nerve, fat, liver, and fibroblast cell lines by forced expression of MyoD. Proceedings of the National Academy of Sciences of the United States of America. 1989;86(14):5434-5438.
10. Wright WE, Sassoon DA, Lin VK. Myogenin, a factor regulating myogenesis, has a domain homologous to MyoD. Cell. 1989;56(4):607-617.
11. Kassar-Duchossoy L, Gayraud-Morel B, Gomès D, Rocancourt D, Buckingham M, Shinin V, et al. Mrf4 determines skeletal muscle identity in Myf5:Myod double-mutant mice. Nature. 2004;431(7007):466-471.

12. Kayalar C, Wong WT. Metalloendoprotease inhibitors which block the differentiation of L6 myoblasts inhibit insulin degradation by the endogenous insulin-degrading enzyme. J Biol Chem. 1989;264(15):8928-8934.
13. Epting CL, King FW, Pedersen A, Zaman J, Ritner C, Bernstein HS. Stem cell antigen-1 localizes to lipid microdomains and associates with insulin degrading enzyme in skeletal myoblasts. Journal of cellular physiology. 2008;217(1):250-260.
14. Tundo GR, Sbardella D, Ciaccio C, Grasso G, Gioia M, Coletta A, et al. Multiple functions of insulin-degrading enzyme: a metabolic crosslight? Crit Rev Biochem Mol Biol. 2017;52(5):554-582.
15. Duckworth WC, Bennett RG, Hamel FG. Insulin degradation: progress and potential. Endocr Rev. 1998;19(5):608-624.
16. Kurochkin IV. Insulin-degrading enzyme: embarking on amyloid destruction. Trends Biochem Sci. 2001;26(7):421-425.
17. Harada S, Smith RM, Smith JA, Jarett L. Inhibition of insulin-degrading enzyme increases translocation of insulin to the nucleus in H35 rat hepatoma cells: evidence of a cytosolic pathway. Endocrinology. 1993;132(6):2293-2298.
18. Farris W, Mansourian S, Chang Y, Lindsley L, Eckman EA, Frosch MP, et al. Insulin-degrading enzyme regulates the levels of insulin, amyloid beta-protein, and the beta-amyloid precursor protein intracellular domain in vivo. Proceedings of the National Academy of Sciences of the United States of America. 2003;100(7):4162-4167.
19. Meneses MJ, Borges DO, Dias TR, Martins FO, Oliveira PF, Macedo MP, et al. Knockout of insulin-degrading enzyme leads to mice testicular morphological changes and impaired sperm quality. Mol Cell Endocrinol. 2019;486:11-17.
20. Livak KJ, Schmittgen TD. Analysis of relative gene expression data using real-time quantitative PCR and the 2(-Delta Delta C(T)) Method. Methods (San Diego, Calif). 2001;25(4):402-408.
21. Li H, Wu J, Zhu L, Sha L, Yang S, Wei J, et al. Insulin degrading enzyme contributes to the pathology in a mixed model of Type 2 diabetes and Alzheimer's disease: possible mechanisms of IDE in T2D and AD. Bioscience reports. 2018;38(1).
22. Yokono K, Imamura Y, Shii K, Mizuno N, Sakai H, Baba S. Immunochemical studies on the insulin-degrading enzyme from pig and rat skeletal muscle. Diabetes. 1980;29(10):856-859.
23. Bondy CA, Zhou J, Chin E, Reinhardt RR, Ding L, Roth RA. Cellular distribution of insulin-degrading enzyme gene expression. Comparison with insulin and insulin-like growth factor receptors. J Clin Invest. 1994;93(3):966-973.
24. Yfanti C, Mengele K, Gkazepis A, Weirich G, Giersig C, Kuo WL, et al. Expression of metalloprotease insulin-degrading enzyme insulysin in normal and malignant human tissues. Int J Mol Med. 2008;22(4):421-431.
25. Le Grand F, Rudnicki MA. Skeletal muscle satellite cells and adult myogenesis. Curr Opin Cell Biol. 2007;19(6):628-633.

26. Conboy IM, Rando TA. The regulation of Notch signaling controls satellite cell activation and cell fate determination in postnatal myogenesis. Dev Cell. 2002;3(3):397-409.
27. Yablonka-Reuveni Z, Rudnicki MA, Rivera AJ, Primig M, Anderson JE, Natanson P. The transition from proliferation to differentiation is delayed in satellite cells from mice lacking MyoD. Dev Biol. 1999;210(2):440-455.
28. Asakura A, Hirai H, Kablar B, Morita S, Ishibashi J, Piras BA, et al. Increased survival of muscle stem cells lacking the MyoD gene after transplantation into regenerating skeletal muscle. Proceedings of the National Academy of Sciences of the United States of America. 2007;104(42):16552-16557.
29. Steelman CA, Recknor JC, Nettleton D, Reecy JM. Transcriptional profiling of myostatin-knockout mice implicates Wnt signaling in postnatal skeletal muscle growth and hypertrophy. FASEB J. 2006;20(3):580-582.
30. Welle S, Bhatt K, Pinkert CA, Tawil R, Thornton CA. Muscle growth after postdevelopmental myostatin gene knockout. American journal of physiology Endocrinology and metabolism. 2007;292(4):E985-991.
31. Gu H, Cao Y, Qiu B, Zhou Z, Deng R, Chen Z, et al. Establishment and phenotypic analysis of an Mstn knockout rat. Biochem Biophys Res Commun. 2016;477(1):115-122.
32. Lv Q, Yuan L, Deng J, Chen M, Wang Y, Zeng J, et al. Efficient Generation of Myostatin Gene Mutated Rabbit by CRISPR/Cas9. Scientific reports. 2016;6:25029.
33. Kim GD, Lee JH, Song S, Kim SW, Han JS, Shin SP, et al. Generation of myostatin-knockout chickens mediated by D10A-Cas9 nickase. FASEB J. 2020;34(4):5688-5696.
34. Grobet L, Martin LJ, Poncelet D, Pirottin D, Brouwers B, Riquet J, et al. A deletion in the bovine myostatin gene causes the double-muscled phenotype in cattle. Nat Genet. 1997;17(1):71-74.
35. Kambadur R, Sharma M, Smith TP, Bass JJ. Mutations in myostatin (GDF8) in double-muscled Belgian Blue and Piedmontese cattle. Genome Res. 1997;7(9):910-916.
36. Qian L, Tang M, Yang J, Wang Q, Cai C, Jiang S, et al. Targeted mutations in myostatin by zinc-finger nucleases result in double-muscled phenotype in Meishan pigs. Scientific reports. 2015;5:14435.
37. Bi Y, Hua Z, Liu X, Hua W, Ren H, Xiao H, et al. Isozygous and selectable marker-free MSTN knockout cloned pigs generated by the combined use of CRISPR/Cas9 and Cre/LoxP. Scientific reports. 2016;6:31729.
38. Crispo M, Mulet AP, Tesson L, Barrera N, Cuadro F, dos Santos-Neto PC, et al. Efficient Generation of Myostatin Knock-Out Sheep Using CRISPR/Cas9 Technology and Microinjection into Zygotes. PloS one. 2015;10(8):e0136690.
39. Wang X, Niu Y, Zhou J, Zhu H, Ma B, Yu H, et al. CRISPR/Cas9-mediated MSTN disruption and heritable mutagenesis in goats causes increased body mass. Anim Genet. 2018;49(1):43-51.
40. He Z, Zhang T, Jiang L, Zhou M, Wu D, Mei J, et al. Use of CRISPR/Cas9 technology efficiently targetted goat myostatin through zygotes microinjection resulting in double-muscled phenotype in goats. Bioscience reports. 2018;38(6).

41. Thomas M, Langley B, Berry C, Sharma M, Kirk S, Bass J, et al. Myostatin, a negative regulator of muscle growth, functions by inhibiting myoblast proliferation. J Biol Chem. 2000;275(51):40235-40243.
42. Ge L, Dong X, Gong X, Kang J, Zhang Y, Quan F. Mutation in myostatin 3'UTR promotes C2C12 myoblast proliferation and differentiation by blocking the translation of MSTN. International journal of biological macromolecules. 2020;154:634-643.

Figures

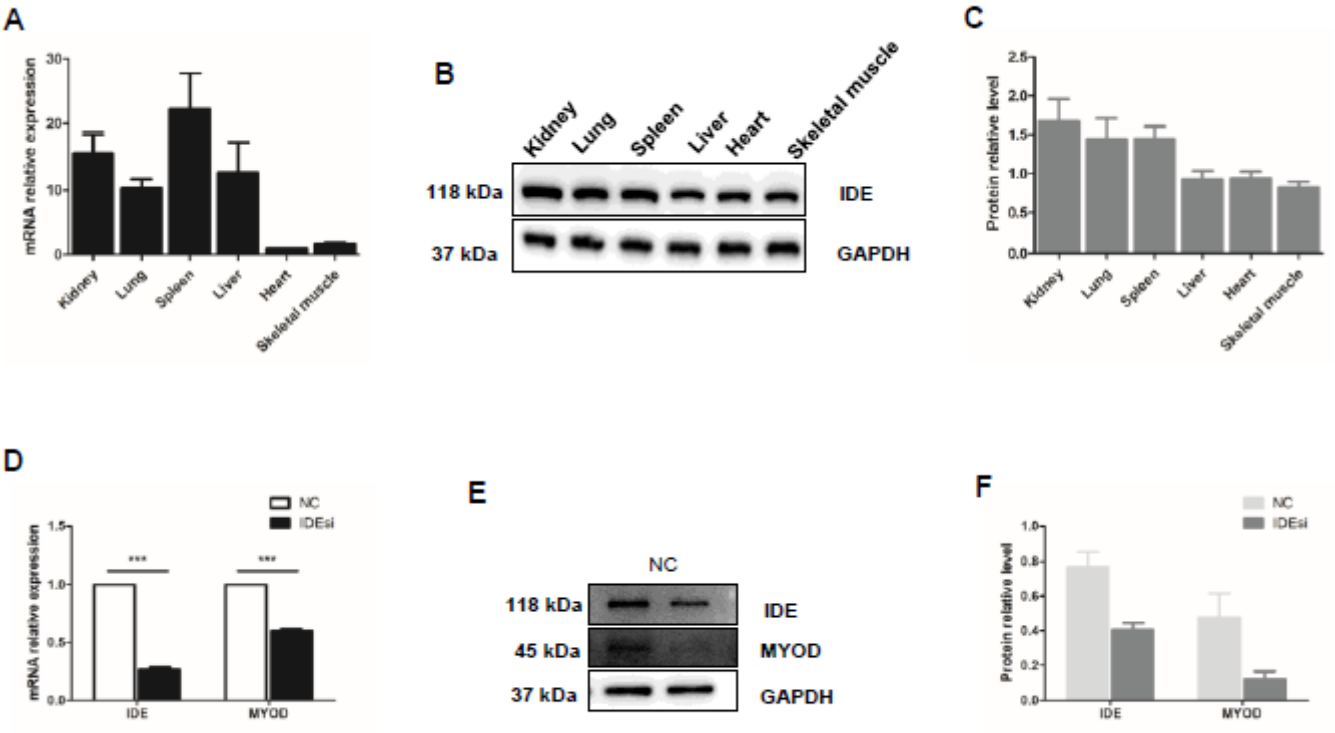

Figure 1

IDE is widely expressed in pig tissues and its knockdown reduces MYOD expression. (A-C) RT-qPCR assay (A) and Western blotting analysis (B-C) indicate that IDE is widely expressed in kidney, lung, spleen, liver, heart, and skeletal muscle of pigs. (D-F) IDE knockdown reduces IDE and MYOD expression in both mRNA (D) and protein level (E-F) with RT-qPCR assay and Western blotting analysis, respectively. ***P < 0.001.

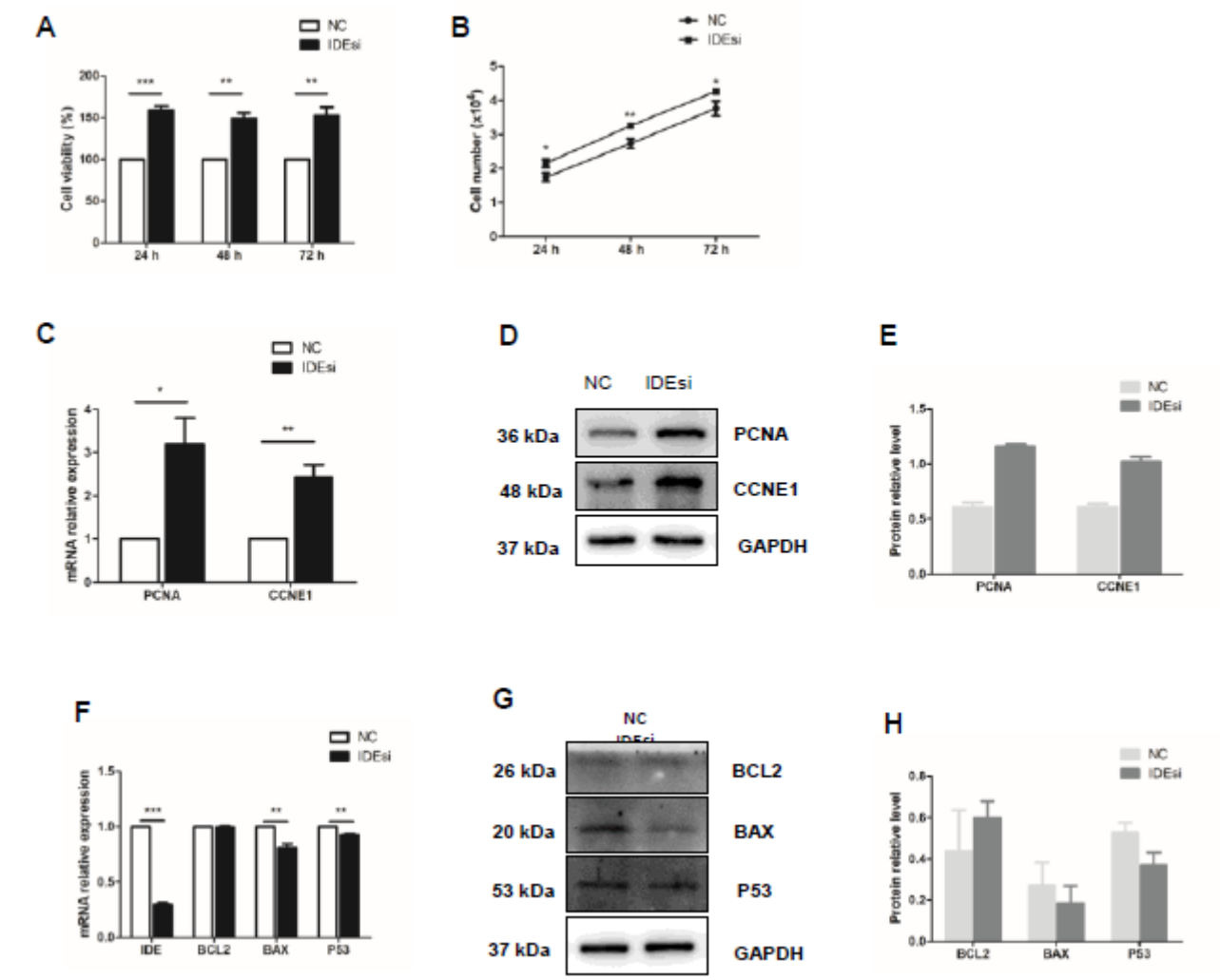

Figure 2

Downregulation of IDE promotes the proliferation and mitigates the apoptosis of porcine skeletal muscle stem cells (PSMSCs). (A) CCK-8 assay shows that cell viability is increased in IDEsi group than that in NC group after transfection into PSMSCs for 24 h, 48 h, and 72 h. (B) IDE knockdown increases cell number compared with NC group after transfection into the same number of PSMSCs for 24 h, 48 h, and 72 h. (C-E) mRNA relative expression (C) and protein levels (D-E) of PCNA and CCNE1 of PSMSCs are increased in IDEsi group than those in NC group via RT-qPCR assay and western blotting analysis, respectively. (F) RT-qPCR assay shows that IDE knockdown decreases mRNA relative expression of IDE, BAX, and P53, but has no significant effect on the expression of BCL2 mRNA. (G-H) The protein levels of BAX and P53 but not BCL2 of PSMSCs are declined in IDEsi group than those in NC group. *P < 0.05, **P < 0.01, and ***P < 0.001.

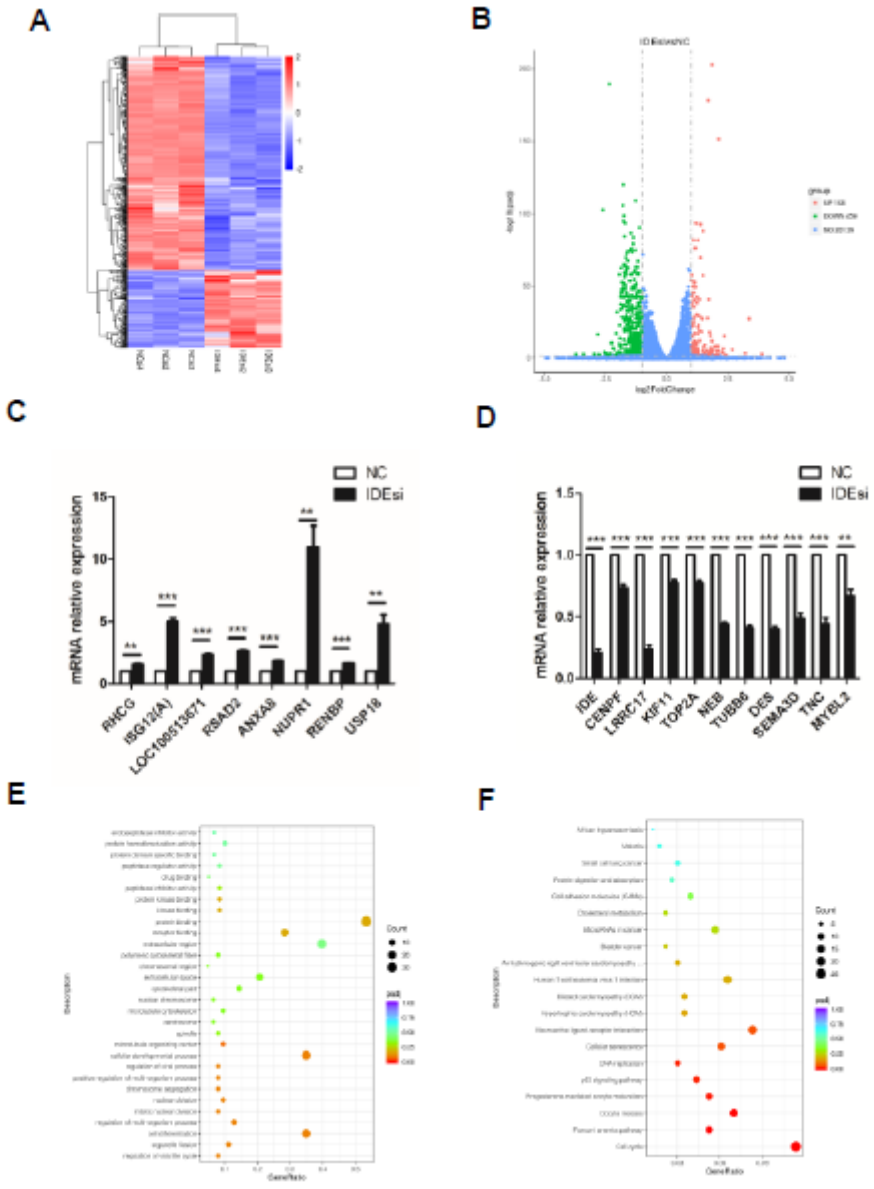

Figure 3

RNA sequencing (RNA-seq) analysis identifies 627 differentially expressed genes (DEGs) with adjusted P<0.05, |log2 fold change| >=1. (A) Heatmap of RNA-seq shows clusters of DEGs in the PSMSCs from IDEsi group and NC group. (B) The volcano plot shows 168 up-regulated DEGs and 459 down-regulated DEGs in IDEsi-transfected PSMSCs compared with NC-transfected PSMSCs. (C-D) The mRNA relative expression of randomly selected 8 up-regulated DEGs (C) and 10 down-regulated DEGs (D) from RNA-seq are confirmed by RT-qPCR assay. (E) GO analysis of all DEGs shows each top10 terms of biological process, cellular component, and molecular function. (F) KEGG pathway analysis of all DEGs shows top 20 pathways. **P < 0.01, and ***P < 0.001.

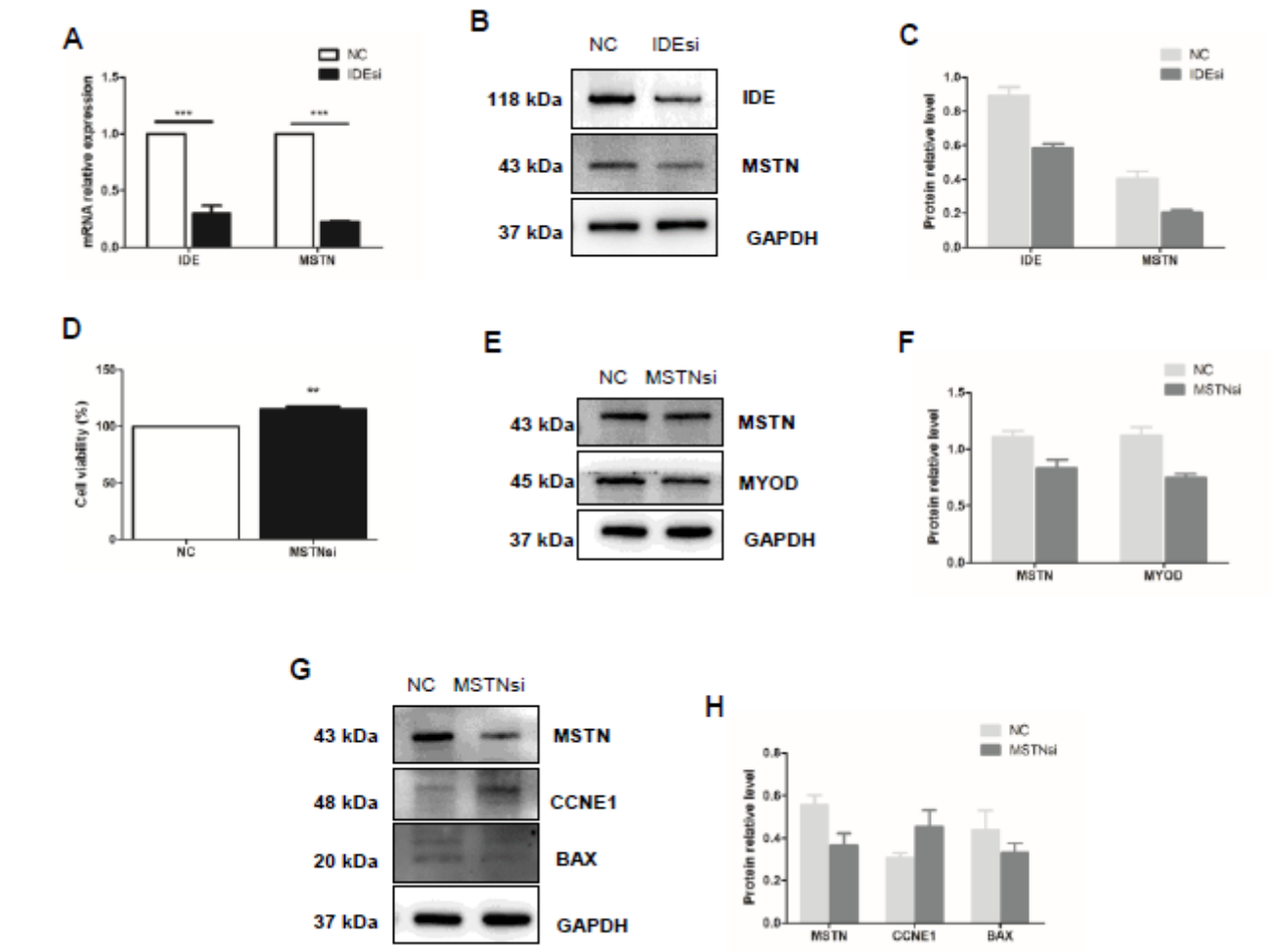

Figure 4

IDE regulates PSMSCs through MSTN/MYOD pathway. (A) One of down-regulated DEGs, MSTN, is confirmed its downregulation in PSMSCs transfected with IDEsi for 48 h compared with that in NC group PSMSCs in both mRNA (A) and protein levels (B-C) via RT-qPCR assay and western blotting analysis, respectively. (D) CCK-8 assay shows that cell viability is increased in MSTNsi group than that in NC group after transfection into PSMSCs for 48 h. (E-F) MSTN knockdown reduces the protein levels of MSTN and MYOD in PSMSCs. (G-H) Downregulation of MSTN leads to increase in the protein level of CCNE1 and decrease in the protein levels of MSTN and BAX in PSMSCs. **P < 0.01, and ***P < 0.001.

Supplementary Files

This is a list of supplementary files associated with this preprint. Click to download.

- Additionalfile1.docx